Chapter 2
Capacity Analysis

The capacity analysis is one of the most important methods to demonstrate the system performance. The methods used for analyzing the system capacity include Shannon capacity analysis, outage capacity analysis and cutoff capacity etc. For actual system analysis, the throughput or user number capacity analysis is usually considered. In this chapter, Shannon capacity analysis for Group Cell will be introduced. Multi-user diversity (MUD) can also be used in Group Cell architecture to improve the system capacity. The capacity maximization method with peak-power constraints for cooperative communications will be illustrated.

2.1 Capacity Analysis of Single-User in Group Cell

We will analyze the Shannon capacity of fixed Group Cell structure [1] and slide Group Cell structure in the scenario that each antenna's transmission power is equal. There is still another transmission power allocation method—weighted power transmission scheme [2], which is analyzed in other works. The outage capacity performance analyses will be introduced in Sect. 2.1.2.

2.1.1 Shannon Capacity Analyses of Group Cell

2.1.1.1 Single Group Cell without Shadow Fading

If there is no shadow fading in consideration, the cell selection is only based on the path loss. In a single Group Cell with N antennas, the received power in downlink is $P_r = \sum_{i=1}^{N} P_t L_i$ where P_t is the transmitted power that is equally allocated by each antenna and L_i is the path loss between the antenna and Mobile Terminal (MT).

X. Tao et al., *Group Cell Architecture for Cooperative Communications*,
SpringerBriefs in Computer Science, DOI: 10.1007/978-1-4614-4319-3_2,

If neighboring cell interferences are neglected, the Shannon capacity using equal transmission power scheme can be derived by Shannon formula, which represents an upper bound of the reliable bit transmission rate with limited bandwidth B and the noise power density N_0:

$$C = B \log_2(1 + \sum_{i=1}^{N} P_{t,i} L_i / N_0 B) \tag{2.1}$$

The average channel capacity of Group Cell is:

$$C_{AVG} = \iint_S p(x,y) B \log_2(1 + \sum_{i=1}^{N} P_t L_i(x,y)/N_0 B) dxdy \tag{2.2}$$

where S is the coverage area of the Group Cell and $p(x,y)$ is the probability density function (PDF) of the MT's location in position $z = (x,y)$.

2.1.1.2 Multi-Group Cell with Shadow Fading

In a single Group Cell scenario, the path loss with shadow fading is $L_i^{'} = L_i \times L_{shadow}$, where $L_{shadow} = 10^{-N(0,\sigma^2)/10}$ and σ is the standard deviation of the shadow fading.

Considering Multi-Group Cell scenario, the shadow fading has impacts on the Group Cell selection. For analyzing this effect, a Monte Carlo simulation is used in Multi-Group Cell scenario with center cell consideration only. Equivalent path-loss (EPL) is used as an index of a selected cell.

$$L_{k,EP}^{'} = \sum_{i=1}^{N} L_{k,i}^{'} = \sum_{i=1}^{N} L_{k,i} \times L_{i,shadow} \tag{2.3}$$

where $L_{k,i}^{'}$ is co-operation of path-loss and shadow fading between user and the ith antenna of kth Group Cell.

So, (2.2) can be deduced to:

$$C_{AVG} \approx \frac{\iint_{S, EPL_0 > EPL_k, \forall k \neq 0} B \log_2(1 + P_r/N_0 B)\, dxdy}{\left(\frac{9\sqrt{3}}{2} r\right)^2} \tag{2.4}$$

where S is the research area, r is the radius of the Group Cell, EPL_k is the EPL of the kth Group Cell and EPL_0 is the largest of EPL_k.

2.1.1.3 Performance Analysis and Evaluation

The main characteristics for the simulation, used in MATLAB, of the Group Cell architecture and traditional cellular structure are summarized in Table 2.1.

Table 2.1 Simulation parameters of single-user group cell

Parameters	Settings
Group cell size	3
Number of group cells	9
Carrier frequency	5.3 GHz
Total transmission power of AP/BS	43 dBm
Total bandwidth	10 MHz
Bandwidth allocated to each user	100 kHz
Radius of cell	500 m
Thermal noise	−145 dBw
Standard deviation of shadow fading	5 dB

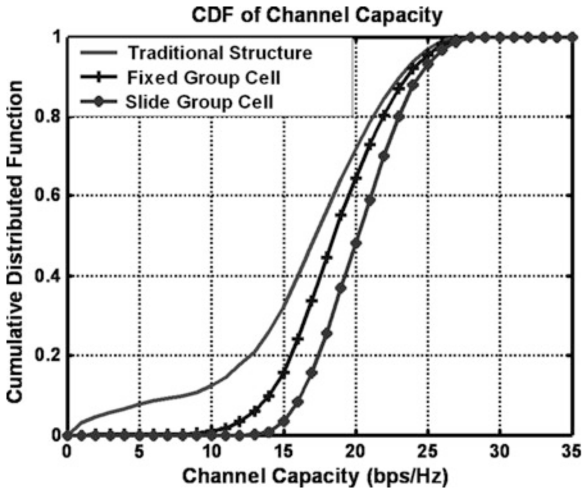

Fig. 2.1 Channel capacity of group cell vs. traditional structure

The simulation results are shown in Fig. 2.1, which indicates the cumulative distribution function (CDF) of channel capacity of traditional cellular structure, fixed Group Cell and slide Group Cell structure respectively.

Figure 2.1 shows the gain of channel capacity brought by Group Cell architecture. We can see from the CDF curve that fixed Group Cell can achieve about 50 % gain compared to traditional cellular structure and the slide Group Cell can further achieve 30 % gain vs. fixed Group Cell. The total transmission power of an AP in Group Cell architecture and a BS in tradition structure is equal and the multi-user interferences are ignored in this simulation.

2.1.2 Outage Capacity Analysis of Group Cell

In order to evaluate the coverage performance of Group Cell, we analyze the outage performance [3] of a Group Cell and traditional cellular structure. The outage probability is defined as the probability when received signal to noise ratio

(SNR) is smaller than the target SNR. In this section, we only focus on the analyses of downlink outage performance as an example. Moreover, we assume that the system is free from user interference. As there are more than one antennas that transmit signals to the user in downlink, we normalize the whole power allocated to the user for maintaining the fairness to traditional cellular structure with single antenna.

Based on the power distribution function of Rayleigh-Log-Normal channel model [4]:

$$f_\gamma(\gamma|u,\sigma) = \int_0^\infty \frac{1}{s} e^{-\frac{\gamma}{s}} \frac{10}{\ln(10)\sqrt{2\pi}\sigma s} \exp\{-\frac{(10\log_{10} s - u)^2}{2\sigma^2}\} ds \tag{2.5}$$

The outage probability of single antenna system (N = 1) can be deduced as follows:

$$\begin{aligned} P_{otg,N=1} &= P\{\gamma < \gamma_{req}|\mu,\sigma\} \\ &= \iint_S F_\gamma(\gamma|s,u,\sigma) P\{s = (x,y)|\mu,\sigma\} ds \\ &\approx \iint_S \frac{p(s)}{\sqrt{\pi}} \sum_{i=1}^{N_H} A_i g(x_i,\gamma|\mu,\sigma) ds \end{aligned} \tag{2.6}$$

Assuming the SNR at the transmit end (Group Cell with N single antennas) is γ_t, the received signals at the MT will be presented as:

$$\gamma_{rec} = \gamma_t \sum_{i=1}^{N} G_i \tag{2.7}$$

where G_i is the path gain of the link between the ith antenna and MT. If $\gamma_t = 1$,

$$\begin{aligned} P_{otg} = &\int_{-\infty}^{+\infty} \cdots \int_{-\infty}^{\infty} \frac{1}{\pi^{N/2}} e^{-\sum_{i=1}^{N} x_i^2} \\ &\{1 - \sum_{i=1}^{N} e^{-\eta\phi_i} \prod_{n \neq i} \frac{\phi_n}{\phi_n - \phi_n}\} dx_1 dx_2 \cdots dx_N \end{aligned} \tag{2.8}$$

where $\phi_i = 10^{-(\sqrt{2}\sigma x_i + u_i)/10}$.

Different transmission power allocation methods will have different outage performances. In this section, we only analyzed the equal transmission power allocation scheme like the capacity analysis in Sect. 2.1.1.

With equal transmission power allocation scheme in downlink, each antenna of N total antennas uses equal transmission power to transmit signals. From (2.6) and (2.8), the outage probability of equal transmission power allocation scheme can be expressed as:

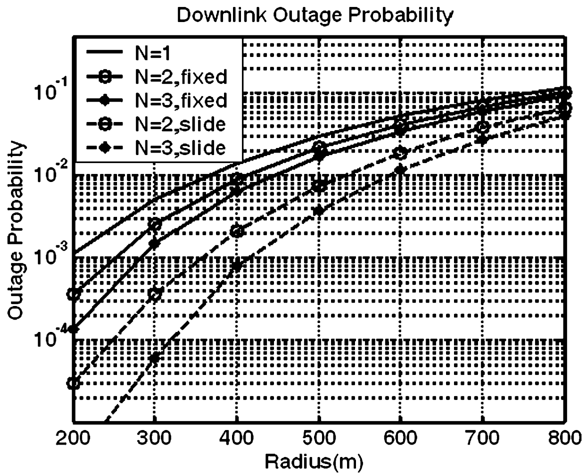

Fig. 2.2 Downlink outage performance with equal transmission power allocation scheme

$$P_{otg} = \int_{-\infty}^{+\infty} \cdots \int_{-\infty}^{\infty} \frac{1}{\pi^{N/2}} e^{-\sum_{i=1}^{N} x_i^2} \bullet \{1 - \sum_{i=1}^{N} e^{-\eta\phi_i} \prod_{n\neq i} \frac{10^{-(\sqrt{2}\sigma x_k+u_k)/10}}{10^{-(\sqrt{2}\sigma x_k+u_k)/10} - 10^{-(\sqrt{2}\sigma x_i+u_i)/10}}\} dx_1 dx_2 \cdots dx_N \tag{2.9}$$

Using multiple Gauss-Hermite integral method, the outage performance of the Group Cell can be derived. We have used Matlab to perform these calculations. The basic parameters of simulation are same as given in Table 2.1. We have analyzed the outage performance of the Group Cell when the size of Group Cell is 1, 2 and 3. The situation of 1 cell in the Group Cell is equal to l traditional cellular structure. The simulation results are shown in Fig. 2.2.

It indicates the numerical results of outage performances of fixed and slide Group Cell using equal transmission power allocation scheme in downlink. The figure verifies the merits of Group Cell from the aspect of coverage performance. From the simulation results, we can see that in order to get 1e-2 outage probability, the cell radius of fixed and slide Group Cell of 2 antennas reaches 420 m and 540 m respectively while the cell radius of traditional cellular structure is less than 400 m. When the size of Group Cell reaches to 3, the cell radius of fixed and slide Group Cell structure extends even further.

2.2 Capacity Analysis with Multi-User Diversity in Group Cell

Section 2.1 analyzed the channel capacity and outage performance of the Group Cell architecture. Moreover, MUD is convincingly an effective method to improve system throughput at a large scale. The MUD can be achieved by proper scheduling algorithms in actual mobile communication systems, such as the Maximal C/I algorithm, Proportional Fairness algorithm and so on [5]. But in multi-antenna systems, such as the Group Cell architecture, how to use the MUD is still the emphasis of research activities. There are still several unanswerable questions in this research area, such as the multi-dimensional resource scheduling and allocation, the feedback of user current information and the method of maximizing MUD etc. In this section, we will utilize the MUD strategy in Group Cell and analyze the system performance of the capacity gain brought by MUD strategy.

Consider the scenario of MUD strategy applied in Group Cell architecture. In traditional single antenna cellular environment, by using the strategy of MUD, the capacity of the system will be increased greatly. So, we will analyze the capacity gain in Group Cell architecture with MUD in the following paragraphs. Considering a more universal situation, just like a distributed MIMO [6] case in Group Cell architecture, the result of this analysis will be more useful.

With the strategy of MUD, the system needs to maximize the sum capacity defined as the maximum achievable sum of long-term average data rates transmitted to all users. In the single-input single-output (SISO) case, it has been shown that transmitting to the user with the strongest channel gain in the given time slot is an approach that can achieve the maximum capacity [7]. Therefore for the receivers in SISO system, it is sufficient to feedback their instantaneous SINR to the transmitter. The transmitter then selects the user with the best SINR for transmission.

The challenge of multi-antenna systems is that the link throughput depends on both the received SINR as well as the subspace structure of the channel matrix and the receiver. So, the optimal MUD strategy for allocating antennas and time slots to users is still the hot research area. In this section, we can still use the scheduling algorithms in SISO for multi-user Group Cell architecture. Although this scheduling algorithm for MUD may not be optimal for multi-antenna system, it can still bring the capacity gain at a large scale.

Assume that the transmit end (Group Cell) has Mt antennas and the receive end (MT) has Mr antennas. The system capacity of the distributed MIMO Group Cell architecture can be denoted as:

$$C(Mt, Mr) = \log_2 \det(IMr + \frac{P_r}{N_0 BMt} HH^H) \tag{2.10}$$

where H is a $Mt \times Mr$ complex matrix representing the channel situation between the Mt antennas and Mr antennas. The H^H is the Hermit inverse of H. So, formula will be revised as:

$$C(M_t, M_r)_{AVG} = \iint_S p(x,y) \log_2 \det\left(I_{M_r} + HH^H \frac{\sum_{i=1}^{M_t} P_{t,i} L_i(x,y)}{N_0 BM_t} \right) dxdy \tag{2.11}$$

Moreover, the affection of shadow fading must also be considered because it has some impacts on the power loss and cell selection. Using the customary stationary log-normal model for shadow fading, for all MT position $z = (x, y)$, $L_{shadow} \sim N(0, \sigma^2)$.

The average channel capacity will be:

$$C(M_t, M_r)_{AVG} = \iint_S p(x, y) \log_2 \det\left(I_{M_r} + HH^H \frac{\sum_{i=1}^{M_t} P_{t,i} L_i^{'}(x, y)}{N_0 B M_t} \right) dxdy \quad (2.12)$$

where $L_i^{'}(x, y) = L_i(x, y) \times L_{shadow}$.

Applying the strategy of MUD in the Group Cell, assume that there are K users in a Group Cell. The average channel capacity with MUD will be:

$$C(K, M_t, M_r)_{AVG} = \max_{k=1,2,\ldots,K} \left[\iint_S p(x, y) \log_2 \det\left(I_{M_r} + H_k H_k^H \frac{\sum_{i=1}^{Mt} P_{t,i} L_i^{'}(x, y)}{N_0 B M_t} \right) dxdy \right] \quad (2.13)$$

2.2.1 Calculation of Capacity Gain with MUD

The use of MUD strategy will greatly improve the capacity of Group Cells. Let's analyze the capacity gain brought by MUD in detail.

At first, let's assume a simpler model of MIMO in which number of antennas at the transmitter is equal to the number of antennas at the receiver, which means $Mt = Mr = M$.

So, formula (2.10) will be revised as:

$$C(M) = \sum_{j=1}^{M} \log_2\left(1 + \frac{P_r \lambda_j}{N_0 B M}\right) \quad (2.14)$$

where λ_j is the jth eigenvalue of the matrix $W = HH^H$. So, formula (2.13) will be revised as:

$$C(K, M)_{AVG} = \max_{k=1,2,\ldots,K} \left[\iint_S p(x, y) \sum_{j=1}^{M} \log_2\left(1 + \frac{\lambda_j \sum_{i=1}^{M} P_{k,t,i} L_{k,i}^{'}(x, y)}{N_0 B M} \right) dxdy \right] \quad (2.15)$$

From this formula, the exact capacity gain cannot be calculated in a simple form. But we can analyze its upper bound and lower bound.

Assuming that $\gamma k(x,y) = \sum_{i=1}^{M} P_{k,t,i} L'_{k,i}(x,y) \Big/ N_0 BM$ represents the SNR of the kth user, the formula will be simpler. We can easily get the upper-bound and lower-bound of the average capacity from the formula mentioned above.

$$C(K,M)_{AVG} \le M \max_{k=1,2,\ldots,K} \left(\iint_S p(x,y) \log_2(1 + \lambda_{k,\max} \gamma_k(x,y)) dxdy \right)$$

and

$$C(K,M)_{AVG} \ge M \max_{k=1,2,\ldots,K} \left(\iint_S p(x,y) \log_2(1 + \lambda_{k,\min} \gamma_k(x,y)) dxdy \right) \tag{2.16}$$

where $\lambda_{k,\min}$ and $\lambda_{k,\max}$ are the minimum and maximum eigenvalues of the matrix $W = HkHk^H$ respectively.

Further calculations will require the PDF of $\lambda_{k,\min}$ and $\lambda_{k,\max}$. The PDF of $\lambda_{k,\min}$ can be taken from [8] and it is an exponential distribution with M being its mean. The lower bound of $C(K,M)_{AVG}$ can be deduced further, but the PDF of $\lambda_{k,\max}$ has no determinate form. So, we can use the numerical analysis to obtain the upper bound of $C(K,M)_{AVG}$ in order to get the approximate result of the capacity gain, brought by MUD.

For the lower bound of $C(K,M)_{AVG}$, let's analyze two situations. When $\gamma_k(x,y) \cdot 1$, formula can be revised as:

$$C(K,M)_{AVG} \ge M \max_{k=1,2,\ldots,K} \left(\iint_S p(x,y) \log_2(\lambda_{k,\min} \gamma_k(x,y)) dxdy \right) \tag{2.17}$$

Lemma 1 Consider independently and identically distribute (i.i.d.) random variables $\xi 1, \xi 2, \ldots \xi K$ with CDF $F(\cdot)$ and PDF$f(\cdot)$.

If $\lim_{x\to\infty} \{[1 - F(x)]/f(x)\} = c > 0$, where c is a constant.

Then,

$$\max_{k=1,2,\ldots,K} (\xi_1, \xi_2, \ldots \xi_K) - l_K \xrightarrow{\text{d}} \exp[-\exp(-x/c)]$$

with $F(lK) = \int_{-\infty}^{lK} f(x)dx = 1 - 1/K$.

Furthermore, the value of l_K can be derived from (2.7) that $l_K = \ln K$.

From Lemma 1 and the PDF of $\lambda_{k,\min}$, $\max\limits_{k=1,2,\ldots,K}\left[\lambda_{k,\min}\right] - \ln K$ leads to a variable whose PDF is $\exp[-\exp(-x/c)]$. So, the formula (2.17) can be revised as:

$$C(K,M)_{AVG} \geq M\left(\ln K + \iint\limits_{S} p(x,y)\log_2 \gamma k(x,y)dxdy\right) \tag{2.18}$$

For a comparison with the Group Cell without MUD, the lower bound of a capacity gain of each antenna dimension can be written as:

$$\begin{aligned} Gain_{min} &= \frac{C(K,M)_{AVG}}{M} - C_{AVG} \\ &\geq \left(\ln K + \iint\limits_{S} p(x,y)\log_2 \gamma k(x,y)dxdy\right) \\ &\quad - \iint\limits_{S} p(x,y)\log_2(1+\gamma k(x,y))dxdy \\ &\approx \ln K \end{aligned} \tag{2.19}$$

When $\gamma k(x,y) \to 0$, formula (2.19) can be revised as:

$$C(K,M)_{AVG} \geq M \iint\limits_{S} p(x,y)\gamma k(x,y) \max_{k=1,2,\ldots,K}\left(\lambda_{k,\min}\right)dxdy \tag{2.20}$$

From Lemma 1 and the PDF of $\lambda_{k,\min}$ formula (2.20) can be simplified further.

$$C(K,M)_{AVG} \geq M \ln K \iint\limits_{S} p(x,y)\gamma k(x,y)dxdy \tag{2.21}$$

For a comparison with the Group Cell without MUD, the lower bound of a capacity gain of each antenna dimension is

$$\begin{aligned} Gain_{\min} &= \frac{C(K,M)_{AVG}/M}{C_{AVG}} \geq \frac{\ln K \iint\limits_{S} p(x,y)\gamma k(x,y)dxdy}{\iint\limits_{S} p(x,y)\log_2(1+\gamma k(x,y))dxdy} \\ &\approx \ln K \end{aligned} \tag{2.22}$$

In the following part, we will use the simulation approach to verify the theoretical analysis stated above.

Table 2.2 Simulation parameters of MUD in group cell

Parameters	Settings
Group cell size	3
Number of group cells	9
Carrier frequency	5.3 GHz
Total transmission power of AP/BS	20 W
Total bandwidth	10 MHz
Bandwidth allocated for each user	100 kHz
Radius of cell	500 m
Thermal noise	−145dBw
Standard deviation of shadow fading	5 dB

2.2.2 Performance Analysis and Evaluation

The main characteristics of the simulation for the Generalized Distributed Cellular Architecture—Group Cell are summarized in Table 2.2.

In the simulation, the MT and Group Cell are all deployed with single antenna. The simulation results are shown in Figs. 2.3 and 2.4, which indicates the performance gain of Group Cell vs. traditional cellular structure and the capacity gain brought by MUD, respectively.

Figure 2.3 gives the capacity of Group Cell with MUD. From the simulation results, we can see that the Group Cell capacity with MUD is improved as the number of users increased.

To lend further credence to capacity gain brought by MUD, we plot in Fig. 2.4 with the comparison to the bound $\ln K$. From the simulation results, with the increase of user numbers, the capacity gain brought by MUD follows the bound very well. The slight decrease of MUD gain to $\ln K$ is due to the simulation settings that all single antennas deployed in MT and AP.

2.3 Ergodic Capacity of Group Cell Systems with Power Constraints

The system capacity is a very important requirement from perspective of the system performance viewpoint. The target peak data rate in the downlink is 1 Gb/s for LTE-Advanced and the target peak data rate in the uplink is 500 Mb/s considering the traffic demands in cellular networks. Capacity analysis gives us the direction of how to maximize system capacity according to different situations and based on different criterions. In physical implementations of Group Cell systems, each eNodeB has its own power amplifier in its analog front-end and is limited individually by the linearity of the power amplifier. For example, in the standardization of 3GPP LTE-Advanced, it is emphasized that each eNodeB has its own maximal transmit power of 49 dBm for 40 MHz LTE-A carrier [9].

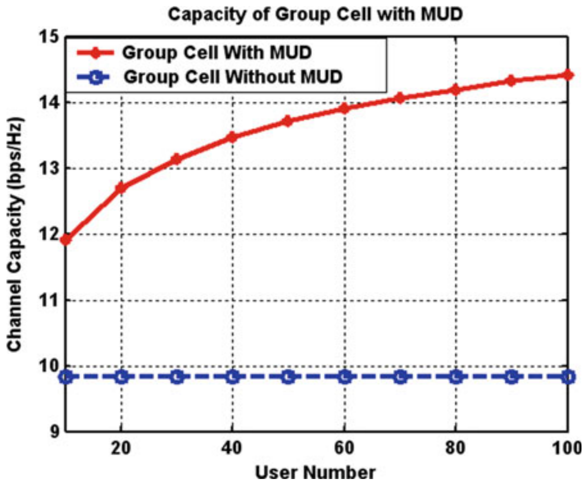

Fig. 2.3 Capacity of group cell with MUD

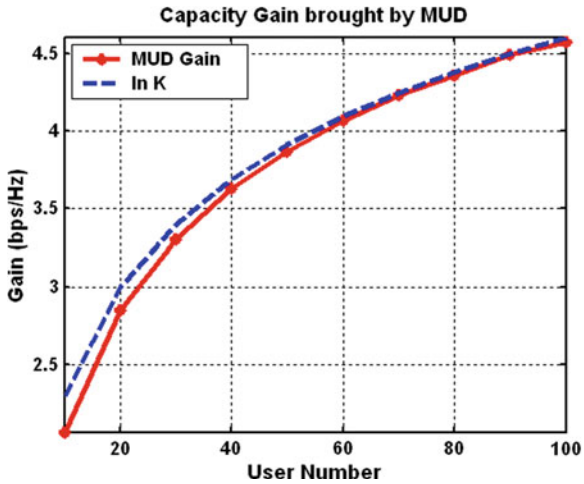

Fig. 2.4 Capacity gain brought by MUD

Furthermore, it is also pointed out that individual peak-power constraints (IPC) must be applied to a group of antennas on each eNodeB [10]. Hence, an IPC on a per-transmit- eNodeB basis is needed for the practical implementation:

$$\mathrm{E}(|\mathbf{X}_i|^2) \leq P_i \quad for\ i = 1, 2, \ldots, N. \tag{2.23}$$

where $\mathbf{X}_i$ denotes the transmitted signal from the ith BS, $\mathrm{E}(\cdot)$ means the expectation operator, and P_i is the ith eNodeB's peak-power constraint.

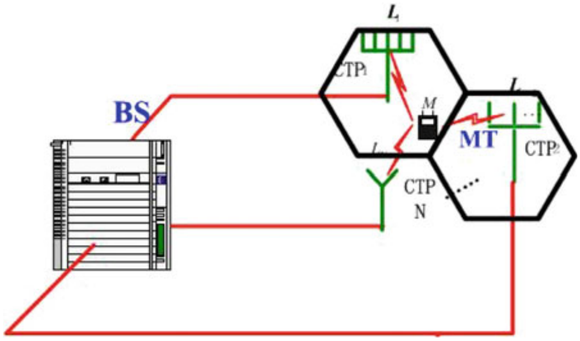

Fig. 2.5 Group cell system model with (N, L_i, M)

2.3.1 System Model and Problem Formulation

The Group Cell system model is shown in Fig. 2.5, which consists of N largely separated coordinated transmission points (CTPs) each with L_i (i = 1, 2,…, N) centralized antennas and one user equipped with M antennas. The channel information is known at transmitter and receiver. Assume each signal transmitted from every CTP arrive at the user simultaneously, the downlink received signal is expressed as

$$\mathbf{Y} = \sum_{i=1}^{N} \sqrt{\eta_i}\mathbf{H}_i\mathbf{X}_i + \mathbf{n} = \mathbf{HX} + \mathbf{n} \tag{2.24}$$

where

1. $\mathbf{X} = (\mathbf{X}_1, \mathbf{X}_2, \ldots, \mathbf{X}_N)^T$ are transmitted signals from N CTPs.
2. $\mathbf{H}_i \in \mathbb{C}^{M \times L_i}$ indicates the small-scale fading from ith CTP to the user, assumed to be frequency-flat fading with zero mean and unit variance; $\mathbf{H} = \left(\sqrt{\eta_1}\mathbf{H}_1 \quad \sqrt{\eta_2}\mathbf{H}_2 \quad \ldots \quad \sqrt{\eta_N}\mathbf{H}_N \right)$ represents a $M \times \sum_{i=1}^{N} L_i$ compound channel;
3. $\mathbf{n} \in \mathbb{C}^{M \times 1}$ is an independent circularly symmetric complex Gaussian noise vector with distribution $\mathcal{CN}(0, \mathbf{I}_M)$;
4. η_i are the parameters related to the SNR

$$\eta_i = \frac{SNR_i}{P_i} \tag{2.25}$$

Where SNR_i is the normalized power ratio of $\mathbf{X}_i$ to the noise (after fading); P_i denotes the individual peak-power constraint of the ith CTP.

This subsection targets the capacity-maximization problem under a more realistic condition, i.e. IPC, in which each BS has its own transmit peak-power constraint. According to (2.24), the instantaneous capacity can be expressed as

$$C = \log\left|\mathbf{I}_M + \mathbf{HQH}^\dagger\right| \overset{(a)}{=} \log\left|\mathbf{I} + \mathbf{QH}^\dagger\mathbf{H}\right| \tag{2.26}$$

where

1. (a) comes from the identity $|\mathbf{I} + \mathbf{AB}| = |\mathbf{I} + \mathbf{BA}|$;
2. $\mathbf{Q}$ is the covariance expression of transmitted signals:

$$\mathbf{Q} = E(\mathbf{XX}^\dagger) = \begin{pmatrix} \mathbf{Q}_{11} & \mathbf{Q}_{12} & \cdots & \mathbf{Q}_{1N} \\ \mathbf{Q}_{21} & \mathbf{Q}_{22} & \cdots & \mathbf{Q}_{2N} \\ \cdots & \cdots & \cdots & \cdots \\ \mathbf{Q}_{N1} & \mathbf{Q}_{N2} & \cdots & \mathbf{Q}_{NN} \end{pmatrix} \tag{2.27}$$

where $\mathbf{Q}_{ij}$ denotes the covariance matrix between signals from the ith and jth CTPs. We consider IPC for each CTP, i.e. $tr(\mathbf{Q}_{ii}) \le P_i$. To maximize the capacity in (2.25), the solution is to optimize the transmit covariance matrix $\mathbf{Q}$, meanwhile the IPC condition is satisfied:

$$\begin{aligned} \{\mathbf{Q}^*\} &= \arg\max C \\ s.t.\ tr(\mathbf{Q}_{ii}) &\le P_i\, for\ i = 1, 2, \ldots N \end{aligned} \tag{2.28}$$

2.3.2 *Capacity Analysis for Group Cell with Power Constraints*

2.3.2.1 Capacity Analysis for (N, L_i, M) Group Cell systems

Since $\mathbf{H}^\dagger\mathbf{H} \in \mathbb{C}^{\sum_{i=1}^N L_i \times \sum_{i=1}^N L_i}$ is a positive semi-definite Hermitian matrix, we can diagonalize it and write $\mathbf{H}^\dagger\mathbf{H} = \mathbf{UDU}^\dagger$ in which $\mathbf{D} \in \mathbb{R}^{\sum_{i=1}^N L_i \times \sum_{i=1}^N L_i}$ is diagonal matrix with descending nonnegative values and $\mathbf{U} \in \mathbb{C}^{\sum_{i=1}^N L_i \times \sum_{i=1}^N L_i}$ is unitary. Thus (2.26) is transformed into

$$C = \log\left|\mathbf{I} + \mathbf{QUDU}^\dagger\right| = \log\left|\mathbf{I} + \mathbf{U}^\dagger\mathbf{QUD}\right| \tag{2.29}$$

Define $\mathbf{S} \triangleq \mathbf{U}^\dagger\mathbf{QU}$, then $\mathbf{Q} = \mathbf{USU}^\dagger$, hence (2.29) becomes $C = \log|\mathbf{I} + \mathbf{SD}|$. Using the Hardamard inequality [11],

$$|\mathbf{I} + \mathbf{SD}| \le \prod_{k=1}^{\sum_{i=1}^N L_i} (1 + S_{kk}D_{kk}) \overset{(a)}{=} \prod_{k=1}^{K} (1 + S_{kk}D_{kk}) \tag{2.30}$$

(a) owes to the fact that $D_{kk} = 0$ for $k > K, rank(\mathbf{H}) = K$. D_{ij} means the element of ith column and jth row in matrix $\mathbf{D}$ and the same is with S_{ij}. As verified in [12], in order to find all solutions to maximize the instantaneous capacity in (2.25), it is sufficient to consider only the class of diagonal, positive semi-definite matrices $\mathbf{S}$ that satisfies $S_{ij} = 0$ for all $i, j > K$. In other words, the solution is to find the matrix $\mathbf{S}$ with the form $\mathbf{S} = \begin{pmatrix} \mathbf{S}_1 & \mathbf{0} \\ \mathbf{0} & \mathbf{0} \end{pmatrix}$, where $\mathbf{S}_1 = diag(S_{kk}),\ k = 1, 2, \ldots, K$. Hence, the capacity-maximization problem is transformed into the following

$$\max_{\{S_{kk}\}_{k=1}^{K}:S_{kk}\geq 0} \sum_{k=1}^{K} \log(1 + S_{kk}D_{kk}) \tag{2.31}$$

Next, we will derive the equivalent transmit peak-power constraints. Divide $\in £^{\sum_{i=1}^{N} L_i \times \sum_{i=1}^{N} L_i}$ into N parts, i.e., let the first L_1 rows of $\mathbf{U}$ to be $\mathbf{u}_1$ and so on. From the expression of $\mathbf{Q} = \mathbf{USU}^{\dagger}$, $\mathbf{Q}$ will be converted into

$$\begin{pmatrix} \mathbf{Q}_{11} & \mathbf{Q}_{12} & \cdots & \mathbf{Q}_{1N} \\ \mathbf{Q}_{21} & \mathbf{Q}_{22} & \cdots & \mathbf{Q}_{2N} \\ \cdots & \cdots & \cdots & \cdots \\ \mathbf{Q}_{N1} & \mathbf{Q}_{N2} & \cdots & \mathbf{Q}_{NN} \end{pmatrix} = \begin{pmatrix} \mathbf{u}_1 \\ \mathbf{u}_2 \\ \cdots \\ \mathbf{u}_N \end{pmatrix} \mathbf{S} \begin{pmatrix} \mathbf{u}_1^{\dagger} & \mathbf{u}_2^{\dagger} & \cdots & \mathbf{u}_N^{\dagger} \end{pmatrix} \tag{2.32}$$

where $\mathbf{u}_i$ is the ith sub-matrix of $\mathbf{U}$ with dimension of L_i rows, hence the IPC condition can be rewritten

$$tr(\mathbf{Q}_{ii}) = tr(\mathbf{u}_i \mathbf{S} \mathbf{u}_i^{\dagger}) = \sum_{k=1}^{K} c_{i,k} S_{kk} \leq P_i \tag{2.33}$$

where $c_{i,k}$ is the non-zero eigenvalue of $\mathbf{u}_i(:,k)\mathbf{u}_i(:,k)^{\dagger}$. $\mathbf{u}_i(:,k)$ means the kth column of $\mathbf{u}_i$ $\ i = 1, 2, \ldots, N$. Therefore the (N, L_i, M) system capacity maximization problem is

$$\begin{aligned} &\max_{\{S_{kk}\}_{k=1}^{K}:S_{kk}\geq 0} \sum_{k=1}^{K} \log(1 + S_{kk}D_{kk}) \\ &s.t.\ tr(\mathbf{u}_i \mathbf{S} \mathbf{u}_i^{\dagger}) = \sum_{k=1}^{K} c_{i,k} S_{kk} \leq P_i,\ i = 1, 2, \ldots, N \end{aligned} \tag{2.34}$$

Obviously, the optimization problem is concave in $\mathbf{S}$, and the constraint condition is convex, thus (2.34) can be solved by convex programming [13].

2.3.2.2 Capacity Analysis for (2, L_i, M) Group Cell Systems

To better elaborate the system's capacity, we derive the explicit solution to maximize capacity for the special case where two BSs cooperate to transmit signals to the user. According to (2.33), the $(2, L_i, M)$ Group Cell system maximal capacity problem can be written as:

$$\begin{aligned} f = &\min_{\{S_{kk}\}_{k=1}^{K}:S_{kk}\geq 0} -\sum_{k=1}^{K}\log(1+S_{kk}D_{kk}) \\ &s.t. \sum_{k=1}^{K} c_{1,k}S_{kk} \leq P_1, \sum_{k=1}^{K} c_{2,k}S_{kk} \leq P_2 \end{aligned} \tag{2.35}$$

It can be solved via Lagrangian function, the Lagrangian function is

$$\begin{aligned} g(\boldsymbol{\lambda},\boldsymbol{\mu}) = &-\sum_{k=1}^{K}\log(1+S_{kk}D_{kk}) - \sum_{k=1}^{K}\lambda_k S_{kk} \\ &+ \mu_1(\sum_{k=1}^{K} c_{1,k}S_{kk} - P_1) + \mu_2(\sum_{k=1}^{K} c_{2,k}S_{kk} - P_2) \end{aligned} \tag{2.36}$$

where both $\boldsymbol{\lambda} = (\lambda_1, \lambda_2, \ldots, \lambda_K)^T$ and $\boldsymbol{\mu} = (\mu_1, \mu_2)^T$ are Lagrange multiplier column vectors associated with the inequality constraints.

The KKT condition is as follows:

$$\begin{cases} -\frac{D_{kk}}{1+S_{kk}D_{kk}} - \lambda_k + \mu_1 c_{1,k} + \mu_2 c_{2,k} = 0 & (a) \\ \lambda_k S_{kk} = 0 & (b) \\ \mu_1(\sum_{k=1}^{K} c_{1,k}S_{kk} - P_1) = 0, \mu_2(\sum_{k=1}^{K} c_{2,k}S_{kk} - P_2) = 0 & (c) \\ S_{kk} \geq 0, \lambda_k \geq 0, \mu_1, \mu_2 \geq 0\ ,\ k = 1, 2, ..., K & (d) \end{cases} \tag{2.37}$$

We aim to find the solution of $\{S_{kk}\}_{k=1}^{K}$, $\boldsymbol{\lambda}$ and $\boldsymbol{\mu}$ via Eq. (2.37). Assume there are K_1 positive values in $\{S_{kk}\}_{k=1}^{K}$. We can define the index set $I = \{k|S_{kk} \neq 0\}$, the size of I is K_1 and the size of $\bar{I}$ is K_2, $K_1 + K_2 = K$. From the equation (a) in (2.37) we get:

$$\mu_1 c_{1,k} + \mu_2 c_{2,k} = \lambda_k + \frac{D_{kk}}{1+S_{kk}D_{kk}} \overset{(*)}{\geq} 0 \tag{2.38}$$

(*) owes to (d) in (2.37), hence $\boldsymbol{\mu} = (\mu_1, \mu_2)^T$ is not zero, i.e., at least one of μ_1 and μ_2 is positive. Therefore there are two cases for obtaining the solution:

A. *Case 1*: *only one of* μ_1 *and* μ_2 *is positive*.

Without loss of generality, assume $\mu_1 = 0$, $\mu_2 \neq 0$

Via derivation of (2.38), we get

$$\mu_2 = \frac{K_1}{P_2 + \sum\limits_{k=1}^{K_1} \frac{c_{2,k}}{D_{kk}}} \tag{2.39}$$

Thus:

(a) for $k \in I$, $S_{kk} = \frac{1}{\mu_2 c_{2,k}} - \frac{1}{D_{kk}}$ and $\lambda_k = 0$.
(b) for $k \notin I$, $S_{kk} = 0$. According to (2.39), there is $\lambda_k = \mu_2 c_{2,k} - D_{kk}$.

Then when $\mu_1 = 0, \mu_2 \neq 0$, the solution $(\mathbf{S}, \boldsymbol{\lambda}, \boldsymbol{\mu})$ is:

$$\begin{aligned} \mathbf{S}^*_{Case1} &= \begin{cases} S_{kk} = \frac{1}{\mu_2 c_{2,k}} - \frac{1}{D_{kk}}, & k \in I \\ S_{kk} = 0, & k \notin I \end{cases} \\ \lambda^*_{Case1} &= \begin{cases} \lambda_k = 0, & k \in I \\ \lambda_k = \mu_2 c_{2,k} - D_{kk}, & k \notin I \end{cases} \\ \mu^*_{1,Case1} &= 0, \quad \mu^*_{2,Case1} = \frac{K_1}{P_2 + \sum_{k=1}^{K_1} \frac{c_{2,k}}{D_{kk}}} \end{aligned} \tag{2.40}$$

The value of K_1 is determined via iterative computation until (d) in (2.37) is satisfied. Via substituting the value of (2.40) in (2.39), we obtain the optimum function value in (2.35):

$$f^*_{opt1} = \sum_{k \in I} \log\Big(\frac{D_{kk}(P_2 + \sum_{k=1}^{K_1} \frac{c_{2,k}}{D_{kk}})}{c_{2,k} K_1}\Big).$$

B. *Case 2*: *none of* μ_1 *and* μ_2 *is zero*.

According to (c) in (2.37), we get:

$$\sum_{k=1}^{K} c_{1,k} S_{kk} = P_1, \ \sum_{k=1}^{K} c_{2,k} S_{kk} = P_2 \tag{2.41}$$

which means both of the two CTPs transmit signals with full power constraint. Via mathematical derivation o (2.40), we get:

(a) for $k \in I$, $\lambda_k = 0$ and $\mu_1 c_{1,k} + \mu_2 c_{2,k} = \frac{D_{kk}}{1 + S_{kk} D_{kk}}$, thus $S_{kk} = \frac{1}{\mu_1 c_{1,k} + \mu_2 c_{2,k}} - \frac{1}{D_{kk}}$;
(b) for $k \notin I$, $S_{kk} = 0$ and $\lambda_k = \mu_1 c_{1,k} + \mu_2 c_{2,k} - D_{kk}$.

So when none of μ_1 and μ_2 is zero, the solution $(\mathbf{S}, \boldsymbol{\lambda}, \boldsymbol{\mu})$ will be

$$\mathbf{S}^*_{Case2} = \begin{cases} S_{kk} = \frac{1}{\mu_1 c_{1,k} + \mu_2 c_{2,k}} - \frac{1}{D_{kk}}, & k \in I \\ S_{kk} = 0, & k \notin I \end{cases}$$
$$\lambda^*_{Case2} = \begin{cases} \lambda_k = 0, & k \in I \\ \lambda_k = \mu_1 c_{1,k} + \mu_2 c_{2,k} - D_{kk}, & k \notin I \end{cases} \tag{2.42}$$

The value of $(\mu^*_{1,Case2}, \mu^*_{2,Case2})$ is chosen to satisfy the peak-power constraints:

$$\begin{cases} \sum_{k=1}^{K} c_{1,k} S_{kk} = \sum_{k \in I} (\frac{c_{1,k}}{\mu_1 c_{1,k} + \mu_2 c_{2,k}} - \frac{c_{1,k}}{D_{kk}}) = P_1 \\ \sum_{k=1}^{K} c_{2,k} S_{kk} = \sum_{k \in I} (\frac{c_{2,k}}{\mu_1 c_{1,k} + \mu_2 c_{2,k}} - \frac{c_{2,k}}{D_{kk}}) = P_2 \end{cases} \tag{2.43}$$

The optimum function value in (2.35) is

$$f^*_{opt2} = \sum_{k \in I} \log(\frac{D_{kk}}{\mu_1 c_{1,k} + \mu_2 c_{2,k}})$$

Conclusion: The maximal capacity of $(2, L_i, M)$ system is $C_{\max} = -\min(f^*_{opt1}, f^*_{opt2})$.

2.3.3 Performance Analysis and Evaluation

Monte Carlo simulations are performed to evaluate the ergodic capacity of Group Cell systems under IPC condition with frequency-flat Rayleigh fading. The mean SNR parameters (namely η_i) play a key role in the simulation.

In the simulations, the user and each BS are equipped with the same number of antennas with $L_i = M = 4 (i = 1, 2, \ldots, N)$; the total power constraint is $P_{total} = 20W$ and each CTP's transmit peak-power is equally confined to $P_i \le P_{total}/N (i = 1, 2, \ldots, N)$.

Figure 2.6 shows the ergodic capacity verse SNR1 for the link of BS1 to the user for different numbers of cooperative BSs. The SNR for the link of BS2 to the user is SNR2. Also the transmit power control (TPC) based water-filling algorithm in [14] is simulated under the same conditions. As shown in Fig. 2.6, the ergodic capacity in Group Cell systems increases with the number of cooperative BSs. The diversity gain due to cooperation among CTPs easily accounts for the result.

Next, Figs. 2.7 and 2.8 illustrate the ergodic capacity for the special case $N = 2$. For comparison, the TPC-based water-filling algorithm and uniform power allocation scheme are also simulated under the same conditions. Figure 2.7 shows that our proposed IPC-based method outperforms the TPC-based uniform power allocation scheme by about 39% when SNR1 = 0 dB, $\eta_2 = \eta_1$.

Fig. 2.6 Ergodic capacity under $L_i = M = 4, \eta_1 = \eta_i$

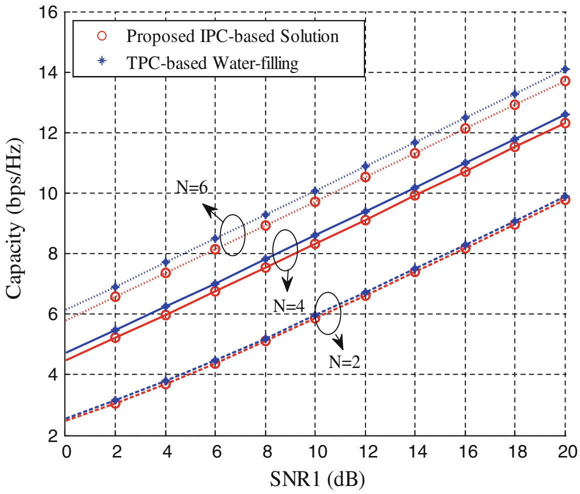

Fig. 2.7 Ergodic capacity under $L_i = M = 4$, $N = 2$, $\eta_1 = \eta_2$

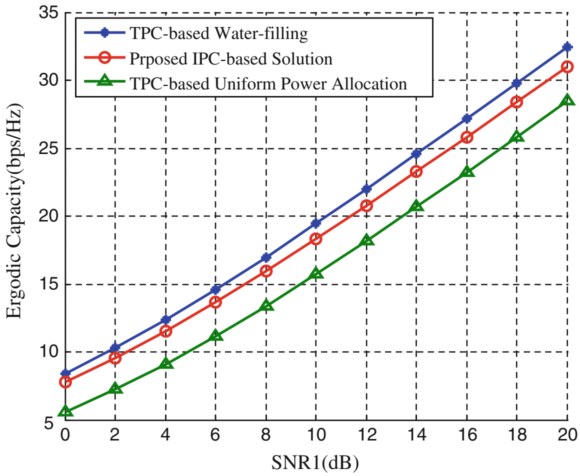

This is because our scheme makes the best use of channel knowledge to realize water-filling under IPC so as to better combat with channel fading. Compared to the TPC-based water-filling, our solution suffers from a little performance loss. The reason is that, the TPC-based water-filling assumes ideal power usage and perfect power cooperation among CTPs. But our IPC-based solution has no power cooperation among BSs, resulting in a less efficient usage of power. However, as each BS must have its own power amplifier in its analog front-end, the IPC is a more realistic condition for practical Group Cell systems. Thereby despite a little performance loss for our solution compared to the TPC-based water-filling, our scheme exhibits more suitability and reliability for Group Cell systems and has more practical implications.

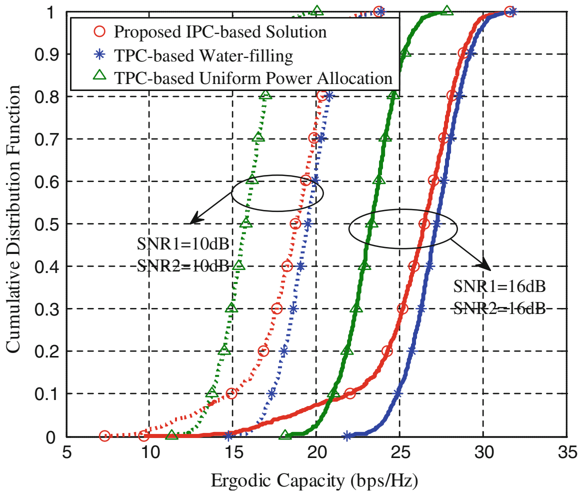

Fig. 2.8 CDF of the capacity under $L_i = M = 4$, $N = 2, \eta_1 = \eta_2$

Figure 2.8 shows the CDF of the ergodic capacity under IPC. It is clear that the capacity offered by our IPC-based solution is better than the TPC-based uniform power allocation, and approaches to the TPC-based water-filling. Similar results are seen in Fig. 2.7 which verifies the simulation analysis from Fig. 2.7.

2.4 Summary

The analyses in Sect. 2.1 showed that the Group Cell architecture can get more superiority than traditional cellular structure in terms of system capacity and coverage. The theoretical analyses in Sect. 2.2 are provided to give the capacity gain bought by MUD and the bottom bound of capacity gain is deduced. In Sect. 2.3, we focused on capacity maximization in Group Cell architecture under individual peak-power constraints for all cooperative transmission nodes. Moreover, our result is achieved under IPC, which is more realistic in practical Group Cell implementations. Simulation results showed that our proposed solution outperforms TPC-based uniform power allocation scheme in terms of the ergodic capacity. Also an elegant tradeoff between system capacity and reality significance can be obtained from our proposed capacity-maximization solution.

http://www.springer.com/978-1-4614-4318-6

Group Cell Architecture for Cooperative Communications
Tao, X.; Cui, Q.; Xu, X.; Zhang, P.
2012, XV, 92 p. 58 illus., Softcover
ISBN: 978-1-4614-4318-6